CHEMICAL ENGINEERING TRANSACTIONS
VOL. 47, 2016
A publication of AIDIC
The Italian Association of Chemical Engineering
Online at www.aidic.it/cet
Guest Editors: Angelo Chianese, Luca Di Palma, Elisabetta Petrucci, Marco Stoller

ISBN 978-88-95608-38-9; **ISSN** 2283-9216
DOI: 10.3303/CET1647002

Synthesis and Characterization of Water Stable ZnO Quantum Dots Based-Sensor for Nitro-Organic Compounds

Marcello Casa[a]*, Maria Sarno[a], Lucia Paciello[a], Marco Revelli Beaumont[b], Paolo Ciambelli[a]

[a]Department of Industrial Engineering and Centre NANO_MATES University of Salerno
Via Giovanni Paolo II ,132 - 84084 Fisciano (SA), Italy
[b]Université Paul Sabatier, 118 Route de Narbonne, 31062 Toulouse Cedex 4, France
mcasa@unisa.it

Here we propose luminescent ZnO QDs synthesized by a simple method in an unusual, powerful and 'green' solvent at low temperature, for the detection of aniline (e.g. 4-nitroanilina) compounds in water environment. To provide aqueous stability, ZnO QDs have been capped by (3-aminopropyl)triethoxysilane (APTES). The synthesized ZnO QDs have been characterized using X-ray diffraction, Transmission Electron Microscopy, Raman, UV-visible, Photoluminescence and Infrared Spectroscopy. This study demonstrates that the as synthesized ZnO QDs are highly luminescent, emitting yellow colour when exposed to UV radiation. Under UV radiation the nanoparticles exhibit high sensitivity to the presence of nitro-compounds in solution when they have a zwitterionic structure, even at very low concentration. In particular, this property makes APTES capped ZnO QDs very effective as sensor for p-nitroaniline.

1. Introduction

Zinc oxide (ZnO) is a white inorganic compound insoluble in water, and the bulk form is widely used as additive in rubbers, plastics, ceramics, glass, cement, lubricants, paints, ointments, adhesives, sealants, pigments, foods, batteries, ferrites, fire retardants, and first-aid tapes (Kołodziejczak-Radzimska and Jesionowski, 2014). In the last years, the synthesis of zinc oxide structures with nano dimension, for example nanorods, nanowires, tetrapods and nanoparticles, has been reported (Xu and Wang, 2011). When ZnO dimensions shrink in the nano domain the material gains new and remarkable physical, antimicrobial and optoelectronic properties that can be useful for electronic, sensoring and biosensoring, spintronic, piezoelectronic applications (Vladimir A Fonoberov, 2006). Among its application, ZnO can be combined with gallium nitride for LED (Bakin et al., 2010), it is the most promising candidate in the field of random lasers to produce an electronically pumped UV laser source (Lu et al., 2015), it is already been used in form of nanorods for gas sensoring of dangerous species like H_2 and CO (Idriss and Barteau, 1992) and is usually used as field emitter (Li et al., 2004). Moreover, ZnO quantum dots (namely nanoparticles of diameter of the order of some nanometers) show strong luminescence and have emerged as a new class of strong fluorescent sensors (Bera et al., 2008). Singh (2012) has studied the effect of ammonia gas on the emission of ZnO decorated luminescent graphene. Various aromatic aldehydes have been selectively detected by Jana (2005) using ZnO QDs. Sharma (2013) have fabricated imine linked ZnO QDs for the detection of Co^{2+} ions. Mg^{2+} ion sensor has been successfully fabricated using ZnO QDs capped with Schiff base (Sharma et al., 2012).

In the last decades, the increasing use of noxious compounds led to devastating effect not only for the environment but also for human health (Kutz et al., 1992). Among various organic and inorganic pollutants, aniline derivatives (e.g. nitroanilines) are suspected carcinogens and are highly toxic to aquatic life. They are toxic by inhalation, in contact with skin and if swallowed. In particular, it has been demonstrated that p-nitroaniline causes methemoglobinemia (B S Kulkarni, 1969), chronic cumulative liver damage (OSHA), and eventually dead (A. Bakdash, 2006). Nevertheless, p-nitroaniline and the other aniline derivatives are widely

Please cite this article as: Casa M., Sarno M., Paciello L., Revelli Beaumont M., Ciambelli P., 2016, Synthesis and characterization of water stable zno quantum dots based-sensor for nitro-organic compounds, Chemical Engineering Transactions, 47, 7-12
DOI: 10.3303/CET1647002

used in the polymer, pharmaceutical, rubber and dye industries (Booth, 2000; *Experimental Organic Chemistry*, 2010).

There are several methods (Gu et al., 1997; Sahori Takeda, 1993) for determination of aniline derivatives, the most common techniques being gas chromatography (GC) (Chiang and Huang, 2008) and high-performance liquid chromatography (HPLC) (Jen et al., 2001). However, these methods involve serious drawbacks such as requirement of drastic conditions, derivatization steps, time consuming and complicated procedure and analysis in non-aqueous medium. Therefore, it is certainly desirable to develop a sensor, easy to be prepared, stable in aqueous media and sensitive to nitroaniline contamination.

Here we report a facile and "green" synthesis of a highly luminescent ZnO-based sensor, stable in water and sensitive to nitroaniline.

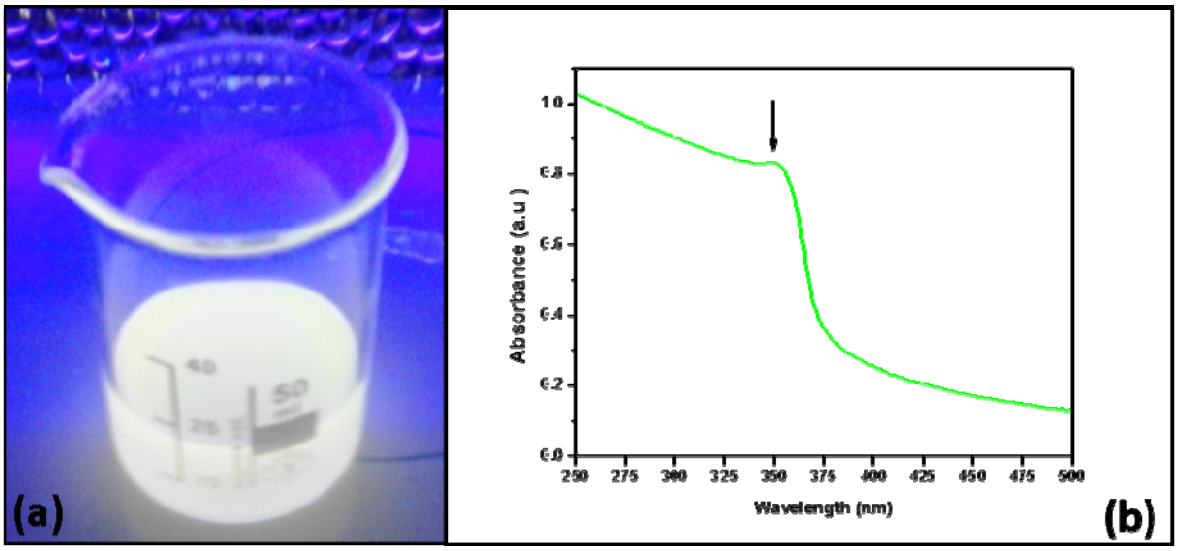

Figure 1: (a) ZnO nanoparticles under UV lamp (b) UV-vis spectrum of ZnO NPs

2. Experimental

2.1 Reagent and Apparatus

Zinc acetate dihydrate (Zn(OAc)2·2H2O, Sigma Aldrich)), 3-aminopropyl triethoxysilane (APTES, Sigma Aldrich), 2-propanol (isopropanol, LC-MS CHROMASOLV®, Sigma Aldrich), ethanol (ACS reagent, ≥99.5%, Fluka Analytical), heptane (anhydrous, 99%, Sigma Aldrich) were used as obtained. 0.05 M NaOH buffer was used for the experiment. Solutions were prepared in double distilled water. TEM images were acquired using a FEI Tecnai electron microscope operating at 200 kV with a LaB6 filament as source of electrons. The samples for TEM observation were casted from volatile solutions on the TEM grid. XRD measurements were performed with a Bruker D8 X-ray diffractometer using CuKa radiation. The KBr technique was applied for determining the FT-IR spectra of the samples, in the scanning range from 4000 to 400 cm^{-1}, by using Vertex 70 instrument (Bruker Corporation). UV-visible spectra were obtained with a Thermo Scientific UV-vis spectrometer.

2.2 Synthesis of ZnO nanoparticles

A 'green' and easy method to prepare ZnO nanoparticles (ZnO NPs) was used. ZnO NPs were synthetized by alkaline hydrolysis of a zinc salt in a non aqueous medium, as described by Hale et al. (2005). We used zinc acetate di-hydrate as metal precursor, and 2-propanol as dispersing phase, as the synthesis of ZnO nanoparticles in isopropanol is easy to control and reproducible, allowing the production of nanoparticles with controlled size. Furthermore, the interactions of the hydroxyl groups of 2-propanol with the surface of the quantum dots hinders nanoparticles agglomeration (Nebukina et al., 2011). In a typical synthesis, 0.1 g of $Zn(CH_3CO_2)_2 \cdot 2H_2O$ was dissolved in 150 ml of isopropanol with heating in a fume hood. Then, the solution was placed in an ice bath, and 15 ml of a chilled solution of NaOH (0.05 M) was added dropwise to isopropanol under stirring. Then, the final solution was placed in a hot bath (50-75 °C). Initially, a solution will contain a large number of small particles or crystals. Because of surface tension, small particles are much more soluble than large particles. The small particles will be precipitated onto larger particles. The small particles therefore act as "nutrients" for bigger particles and the average particle size will increase. The rate of this process, called Ostwald ripening, decreases as the particles grow and the particle size distribution becomes narrower (Hale et al., 2005). After 1 h, a white suspension was obtained, which was centrifuged for 30 min at 7500 rpm to separate the precipitate and then redispersed in isopropanol. To remove impurities from

ZnO NPs, the precipitation-redispersion method proposed by Meulenkamp (1998) in ethanol was first performed in isopropanol. Heptane was added to the ZnO isopropanol colloids. The volume ratio of heptane and isopropanol was 1:1. White ZnO nanoparticles precipitated after a centrifugation of 1 min at 7500 rpm or after a night at 4 °C. After the centrifugation and the removal of the supernatant, the ZnO precipitate was redispersed, again, in a 1:1 mixture of isopropanol and heptane. The above operations were repeated 3 times to reach a small amount of impurities (Sun et al., 2007). To provide aqueous stability to ZnO NPs: (i) 0.015 g of precipitates obtained after washing were dispersed in 19 ml of ethanol; (ii) 2 ml of ethanol containing 0.2 g of APTES, were added dropwise to the suspension; (iii) 0.1 ml of bidistilled water was immediately mixed with the suspension; (iv) the solution was stirred for 1 hour at room temperature, allowing the long-chained APTES molecules to cap ZnO nanoparticles. The APTES capped ZnO NPs were washed by centrifugation and dispersed in water. The solutions obtained gave a yellow emission under UV light (figure 1a).

2.3 Sensoring evaluation

Sensoring properties were evaluated at 25 °C using a UV-spectrometer. The APTES capped ZnO NPs were dispersed in water with a concentration of 0.3 mg/ml. 1 mM p-nitroaniline solution was prepared in bidistilled water. This two solutions were mixed with different volume ratio in order to keep ZnO NPs concentration constant and the concentration of p-nitroaniline ranging from 5 to 37.5 μM and tested.

3. Results and discussion

3.1 UV-vis Spectroscopy

UV-vis spectrum of ZnO NPs (figure 1b) clearly shows shoulder at arounf 350 nm, while the bulk peak of ZnO is located around 380 nm (Wahab et al., 2010). The shoulder position gives evidence that the as-prepared particles are in the nanometer range. In particular, the particle size can be determined from the absorption spectrum using the effective-mass model (Brus, 1992)

$$E_g^* = E_g^{bulk} + \frac{\hbar^2\pi^2}{2r^2}\left(\frac{1}{m_e^* m_e} + \frac{1}{m_h^* m_e}\right) - \frac{1.8e^2}{4\pi\varepsilon\varepsilon_0 r} - \frac{0.124e^4}{\hbar^2(4\pi\varepsilon\varepsilon_0)^2}\left(\frac{1}{m_e^* m_e} + \frac{1}{m_h^* m_e}\right)^{-1}$$

where E_g^* is the band gap energy for the particle, E_g^{bulk} is the bulk band gap energy (for ZnO, E_g^{bulk} = 3.44 eV), ħ is the reduced Planck's constant (h/2π), r is the particle radius, m_e^* is the effective mass of electrons, m_h^* is the effective mass of holes, m_e is the free electron mass, e is the electron charge, ε_0 is the permittivity of free space, and ε is the relative permittivity of the solid. The band gap energy, E_g^*, can be determined from the cut-off wavelength:

$$E_g^* = \frac{h\,c}{\lambda_c}$$

Where h is the Planck's constant and c is the speed of light. The cut off wavelength, λ_c equal to 352 nm is obtained by the peak positions (indicated by the arrow in figure 1b). With this procedure, the evaluated average radius of ZnO NPs is around 4 nm.

3.2 TEM characterization

TEM images of ZnO nanoparticles are presented in figure 2. The particle diameter are in the range 4 - 9 nm, with an average size of 8.3 nm, standard deviation σ =1.7 nm, that fits the results obtained with the effective mass model.

3.3 XRD characterization

The crystallinity of ZnO NPs was confirmed by XRD analysis (figure 3a). In the XRD spectrum of dry ZnO nanoparticles, 7 clear and broad peaks are observed, at 32.17 (001), 34.74 (002), 36.55 (101), 47.94 (102), 56.97 (110), 63.13 (103) and 68.46 (112), respectively. The XRD pattern fits well with a wurtzite structure (Wahab et al., 2010). The average crystal (diameter), evaluated by the Scherrer equation:

$$d = \frac{k\lambda}{\beta \sin\theta}$$

where k is structural constant, λ is the wavelength of X-Ray, d is the size of the nanoparticle and β is full width at half maximum, θ is the Bragg angle. For our evaluation we used the signal of the (102) with 2θ = 47.94°, and the diameter was found to be equal to 8.6 nm. Therefore, the results of TEM, UV-vis, and XRD characterization allow to conclude the ZnO nanoparticles have a radius of around 4 nm.

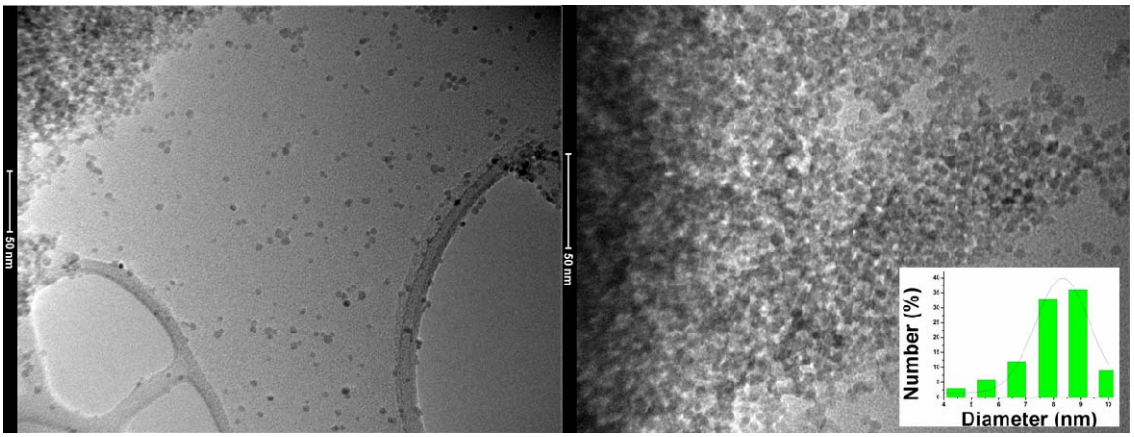

Figure 2: TEM images at different magnification of ZnO NPs and diameter distribution in the insert

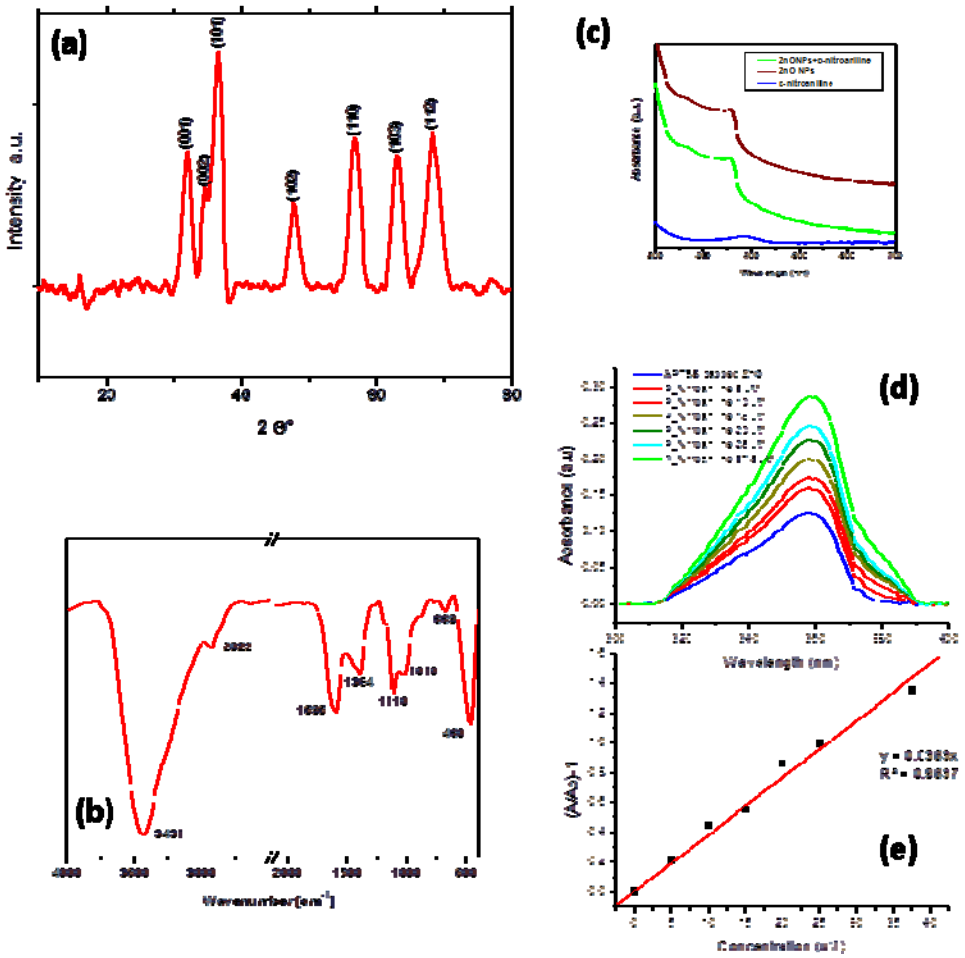

Figure 3: (a) XRD spectrum of ZnO NPs, (b) IR spectra of APTES capped ZnO, (c) UV-vis spectrum comparison of p-nitroaniline, ZnO NPs and ZnO NPs with p-nitroaniline, (d) UV-vis spectrum at different p-Nitroaniline concentration as obtained by baseline subtraction in the range 300-400 nm, (e) UV *peak absorbance vs p-Nitroaniline concentration*

3.4 FT-IR analysis of APTES capped ZnO NPs

FT-IR spectra have been carried out to detect the capping state of APTES molecules on ZnO nanoparticles (Figure 3b). The signals at 3431 and 1595 cm^{-1} correspond to N-H stretching vibration of primary amines on the outer surface of the nanoparticles, the peak at 2922 cm^{-1} is due to the asymmetric stretching vibration of C-H bond, the peak at 1110 cm^{-1} confirms the presence of Si-O-Si groups (polymerization of APTES

molecules), while the peak at 1010 cm^{-1} is due to the presence of C-N bonds, that at 1384 cm^{-1} is attributed to C-H bonds vibration, the peak at 669 cm^{-1} to in plane bending of C-C-C groups, and, finally, the signal at 460 cm^{-1} is due the Zn-O bond (S. Gunasekaran, 2009; Shimanouchi, 1972; Wang et al., 2003). TEM images, not shown here, show the presence of a SiO_2 capping layer around ZnO nanoparticles.

3.5 Interaction of p-nitroaniline with ZnO NPs

UV-vis spectrophotometry has been used to evaluate the effect of p-nitroaniline on the UV absorbance of ZnO. Keeping constant the concentration of ZnO NPs (0.3 mg/ml), the concentration of p-nitroaniline has been varied from 5 to 37.5 μM. Figure 3d shows that the ZnO UV absorbance increases with increasing the aniline concentration. The effect is linear with the analyte concentration as shown in figure 3e:

$$\frac{A}{A_0} - 1 = K \cdot [C]$$

where A_0 is the absorbance evaluated at the shoulder (360 nm) of the spectrum of APTES capped ZnO, A is the absorbance of the contaminated system and C is the concentration of p-nitroaniline. K, evaluated with a regression, has a value of 0.038 μM^{-1}. This behavior is due to the interaction between the zwitterionic structure of p-nitroaniline (stabilized in polar solvent) and the protonated group of APTES shell that allows nanoparticles to retain a larger amount of radiation, indeed figure 3c shows how, at low concentration of p-nitroaniline, the spectra of ZnO NPs with p-nitroaniline does not depend on p-nitroaniline one. On the contrary, this interaction hinders the photoluminescence of ZnO NPs, as shown in figure 4.

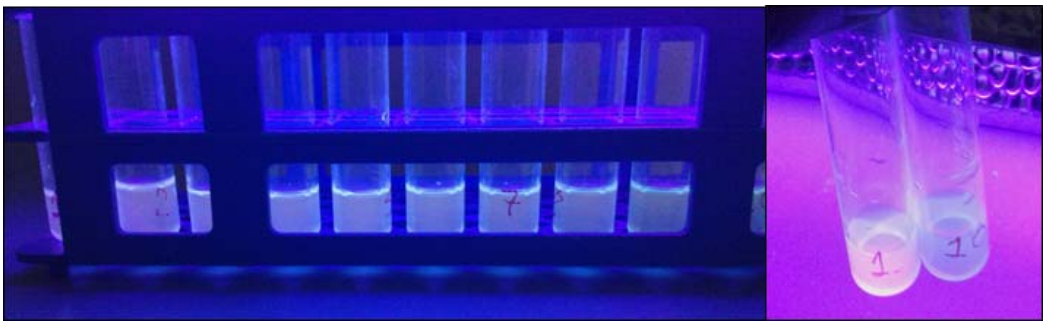

Figure 4: UV emission (under UV lamp) of samples with different concentration of p-nitroaniline on the left and comparison between ZnO luminescence without contaminat (1) and ZnO luminescence with a contaminant concentration of 37.5 μM.

4. Conclusion

APTES-capped ZnO nanoparticles have been tested to detect p-nitroaniline in water. The energy transfer from ZnO NPs to p-nitroaniline results in enhancing the absorbance and quenching the luminescence emission of ZnO NPs. The proposed sensing system has a linear response in the concentration range explored, 5 - 40 μM p-nitroaniline. It is a simple, fast, inexpensive and non-toxic method for trace determination of p-Nitroanilinine in water.

References

A. Bakdash, M.G., 2006. Lethal Poisoning with p-nitroaniline. T + K 73: 61-65.

Bakin, A., Behrends, A., Waag, A., Lugauer, H., Laubsch, A., Streubel, K., 2010. ZnO-GaN Hybrid Heterostructures as Potential Cost-Efficient LED Technology. Proc. IEEE 98, 1281–1287. doi:10.1109/JPROC.2009.2037444

Bera, D., Qian, L., Sabui, S., Santra, S., Holloway, P.H., 2008. Photoluminescence of ZnO quantum dots produced by a sol–gel process. Opt. Mater. 30, 1233–1239. doi:10.1016/j.optmat.2007.06.001

Booth, G., 2000. Nitro Compounds, Aromatic, in: Ullmann's Encyclopedia of Industrial Chemistry. Wiley-VCH Verlag GmbH & Co. KGaA.

Brus, L.E., 1992. Structure and electronic states of quantum semiconductor crystallites. Nanostructured Mater. 1, 71–75. doi:10.1016/0965-9773(92)90055-3

B S Kulkarni, V.N.A., 1969. Methemoglobinemia due to nitro-aniline intoxication. Review of the literature with a report of 9 cases. J. Postgrad. Med. 14, 192–200.

Chiang, J.-S., Huang, S.-D., 2008. Simultaneous derivatization and extraction of anilines in waste water with dispersive liquid-liquid microextraction followed by gas chromatography-mass spectrometric detection. Talanta 75, 70–75. doi:10.1016/j.talanta.2007.10.036

Experimental Organic Chemistry: A Miniscale and Microscale Approach, 5 edition. ed, 2010. . Brooks Cole, Boston, Mass.

Gu, X., Li, C., Qi, X., Zhou, T., 1997. Determination of Trace Aniline in Water by a Spectrophotometric Method After Preconcentration on an Organic Solvent-Soluble Membrane Filter. Anal. Lett. 30, 259–270. doi:10.1080/00032719708002801

Hale, P.S., Maddox, L.M., Shapter, J.G., Voelcker, N.H., Ford, M.J., Waclawik, E.R., 2005. Growth Kinetics and Modeling of ZnO Nanoparticles. J. Chem. Educ. 82, 775. doi:10.1021/ed082p775

Idriss, H., Barteau, M.A., 1992. Photoluminescence from zinc oxide powder to probe absorption and reaction of oxygen, carbon monoxide, hydrogen, formic acid, and methanol. J. Phys. Chem. 96, 3382–3388. doi:10.1021/j100187a037

Jana, N.R., Yu, H., Ali, E.M., Zheng, Y., Ying, J.Y., 2007. Controlled photostability of luminescent nanocrystalline ZnO solution for selective detection of aldehydes. Chem. Commun. 1406–1408. doi:10.1039/B613043G

Jen, J.F., Chang, C.T., Yang, T.C., 2001. On-line microdialysis-high-performance liquid chromatographic determination of aniline and 2-chloroaniline in polymer industrial wastewater. J. Chromatogr. A 930, 119–125.

Kołodziejczak-Radzimska, A., Jesionowski, T., 2014. Zinc Oxide—From Synthesis to Application: A Review. Materials 7, 2833–2881. doi:10.3390/ma7042833.

Kutz, F.W., Cook, B.T., Carter-Pokras, O.D., Brody, D., Murphy, R.S., 1992. Selected pesticide residues and metabolites in urine from a survey of the U.S. general population. J. Toxicol. Environ. Health 37, 277–291. doi:10.1080/15287399209531670

Li, Y.B., Bando, Y., Golberg, D., 2004. ZnO nanoneedles with tip surface perturbations: Excellent field emitters. Appl. Phys. Lett. 84, 3603–3605. doi:10.1063/1.1738174

Lu, Y.-J., Shan, C.-X., Zhou, Z.-X., Wang, Y.-L., Li, B.-H., Qin, J.-M., Ma, H.-A., Jia, X.-P., Chen, Z.-H., Shen, D.-Z., 2015. Electrically pumped random lasers with p-diamond as a hole source. Optica 2, 558. doi:10.1364/OPTICA.2.000558

Meulenkamp, E.A., 1998. Synthesis and Growth of ZnO Nanoparticles. J. Phys. Chem. B 102, 5566–5572. doi:10.1021/jp980730h

Nebukina, E.G., Khokhlov, E.M., Zaporozhets, M.A., Vitukhnovskii, A.G., Gubin, S.P., 2011. A comparative study of the structural and spectral characteristics of ZnO nanoparticles dispersed in isopropanol and polyethylene. Inorg. Mater. 47, 143–147. doi:10.1134/S0020168511020117

Sahori Takeda, S.W., 1993. Separation of aniline derivatives by micellar electrokinetic chromatography. J. Chromatogr. A 653, 109–114. doi:10.1016/0021-9673(93)80397-Q

S. Gunasekaran, R.A., 2009. Computation and interpretation of vibrational spectra on the structure of Nitrazepam using semi-empirical and density functional methods. Int. J. ChemTech Res. 1.

Sharma, H., Kaur, N., Pandiyan, T., Singh, N., 2012. Surface decoration of ZnO nanoparticles: A new strategy to fine tune the recognition properties of imine linked receptor. Sens. Actuators B Chem. 166–167, 467–472. doi:10.1016/j.snb.2012.01.076

Sharma, H., Singh, A., Kaur, N., Singh, N., 2013. ZnO-Based Imine-Linked Coupled Biocompatible Chemosensor for Nanomolar Detection of Co2+. ACS Sustain. Chem. Eng. 1, 1600–1608. doi:10.1021/sc400250s

Shimanouchi, T., 1972. Tables of Molecular Vibrational Frequencies. National Bureau of Standards.

Singh, G., Choudhary, A., Haranath, D., Joshi, A.G., Singh, N., Singh, S., Pasricha, R., 2012. ZnO decorated luminescent graphene as a potential gas sensor at room temperature. Carbon 50, 385–394. doi:10.1016/j.carbon.2011.08.050

Sun, D., Wong, M., Sun, L., Li, Y., Miyatake, N., Sue, H.-J., 2007. Purification and stabilization of colloidal ZnO nanoparticles in methanol. J. Sol-Gel Sci. Technol. 43, 237–243. doi:10.1007/s10971-007-1569-z

Vladimir A Fonoberov, A.A.B., 2006. ZnO quantum dots: Physical properties and optoelectronic applications. J. Nanoelectron. Optoelectron. 1, 19. doi:10.1166/jno.2006.002

Wahab, R., Kim, Y.-S., Lee, D.S., Seo, J.-M., Shin, H.-S., 2010. Controlled Synthesis of Zinc Oxide Nanoneedles and Their Transformation to Microflowers. Sci. Adv. Mater. 2, 35–42. doi:10.1166/sam.2010.1064

Wang, Z., Zhang, H., Zhang, L., Yuan, J., Yan, S., Wang, C., 2003. Low-temperature synthesis of ZnO nanoparticles by solid-state pyrolytic reaction. Nanotechnology 14, 11. doi:10.1088/0957-4484/14/1/303

Xu, S., Wang, Z.L., 2011. One-dimensional ZnO nanostructures: Solution growth and functional properties. Nano Res. 4, 1013–1098. doi:10.1007/s12274-011-0160-7